Available online at www.sciencedirect.com
SCIENCE DIRECT®
ELSEVIER
Earth and Planetary Science Letters 222 (2004) 451–467
EPSL
www.elsevier.com/locate/epsl

Lateral variation in upper mantle viscosity: role of water

Jacqueline E. Dixon[a,*], T.H. Dixon[a], D.R. Bell[b], R. Malservisi[a]

[a] *Rosentiel School of Marine and Atmospheric Science, University of Miami, 4600 Rickenbacker Cswy, Miami, FL 33149, USA*
[b] *Department of Chemistry and Biochemistry and Department of Geological Sciences Arizona State University, Tempe, AZ 85287-1604, USA*

Received 27 August 2003; received in revised form 10 March 2004; accepted 15 March 2004

Abstract

Differences in the viscosity of the earth's upper mantle beneath the western US ($\sim 10^{18}$–10^{19} Pa s) and global average values based on glacial isostatic adjustment and other data ($\sim 10^{20}$–10^{21} Pa s) are generally ascribed to differences in temperature. We compile geochemical data on the water contents of western US lavas and mantle xenoliths, compare these data to water solubility in olivine, and calculate the corresponding effective viscosity of olivine, the major constituent of the upper mantle, using a power law creep rheological model. These data and calculations suggest that the low viscosities of the western US upper mantle reflect the combined effect of high water concentration and elevated temperature. The high water content of the western US upper mantle may reflect the long history of Farallon plate subduction, including flat slab subduction, which effectively advected water as far inland as the Colorado Plateau, hydrating and weakening the upper mantle.

Keywords: mantle; viscosity; Western United States; water

1. Introduction

The viscosity of the Earth's mantle influences a wide variety of geophysical phenomena, including convection, melt extraction, seismic attenuation, and the response of Earth's surface to transient loads such as glaciation and earthquakes. Early models of mantle viscosity, primarily based on observations of post-glacial rebound, assumed radial symmetry and had limited depth resolution. Improvements in data and numerical techniques in the last two decades have enabled resolution of both depth and lateral variations in viscosity, especially in the upper mantle. One dichotomy that has emerged from these studies is that local estimates for upper mantle viscosity in the western US, an active tectonic area ($\sim 10^{18}$–10^{19} Pa s) are significantly lower than global average and large regional estimates based on glacial isostatic adjustment in continental shield areas such as Fennoscandia and the interior of North America ($\sim 10^{20}$–10^{21} Pa s) (Table 1). While these differences in part reflect the thermal contrast between the low heat flow continental interior and higher heat flow western North America, here we suggest that regional differences in the water content of the upper mantle also play an important role.

2. Summary of viscosity estimates

The rheological structure of the mantle may be inferred from the Earth's response to unloading asso-

* Corresponding author. Tel.: +1-305-361-4150; fax: +1-305-361-4632.
E-mail address: jdixon@rsmas.miami.edu (J.E. Dixon).

0012-821X/$ - see front matter © 2004 Elsevier B.V. All rights reserved.
doi:10.1016/j.epsl.2004.03.022

ciated with retreat of Late Pleistocene continental ice sheets, termed glacial isostatic adjustment (GIA). These responses include non-tidal acceleration of Earth rotation (e.g., [1,2]), polar motion (e.g., [3–5]), and surface elevation change, including rapid uplift near de-glaciated regions such as Hudson Bay and Fennoscandia. The elevation data are mainly Holocene relative sea level changes, as recorded by dated geological deposits such as raised beaches (e.g., [6–8]) and present-day elevation change recorded by tide gauges and space geodesy (e.g., [9–11]). Surface changes associated with deglaciation will be influenced by the rheological structure of the upper mantle beneath cratonic areas, since the main forcing function (glaciation/deglaciation) is centered on Precambrian shields (Fennoscandia, Hudson Bay). For simplicity we refer to such models as cratonic, even though they are often considered global average models. Peltier [12] and Lambeck and Johnston [13] give complete reviews.

Kaufmann and Lambeck [14] compare several recent viscosity profiles based on these and related methods. Common features include a strong, elastic lithosphere ~ 50–150 km thick (very high to essentially infinite viscosity), an underlying Maxwell viscoelastic upper mantle down to the 660–670 km discontinuity with relatively uniform properties (viscosity 3×10^{20}–4×10^{21} Pa s), and a lower mantle beneath the 660–670 discontinuity with higher viscosity. Peltier [15] gives a range of 3–5×10^{20} Pa s for the upper mantle in three models (VM-1, 2, 3) constrained by GIA data and assuming a spherically symmetric earth with viscoelastic mantle. Because of the scale of loading, most such models have limited resolution in the uppermost mantle, and there are trade-offs; for example, between the thickness of the elastic lithosphere and the viscosity of the mantle immediately below (e.g., [13]).

The viscosity structure of the western US upper mantle differs significantly from these cratonic models. Kaufmann and Amelung [16] estimate values between 2×10^{17} and 1×10^{18} Pa s in the depth range 75–150 km based on leveling data between 1935–1983 measuring deformation after filling of Lake Mead beginning in 1935. Bills et al. [17] report a viscosity range of 5×10^{17} and 5×10^{19} Pa s for the upper mantle between 75 and 150 km depth based on deformed shorelines of Late Pleistocene Lake Bonneville in response to drying over several thousand years.

Table 1
Selected viscosity estimates for upper mantle[a]

Reference	Loading phenomenon or region	Data[b]	Viscosity (Pa s)
Bills et al. [17] (Fig. 12)	Lake Bonneville (drying)	shoreline elevation	3×10^{18}
Bills et al. [17] (Fig. 11)	Lake Bonneville (drying)	shoreline elevation	3×10^{19}
Kaufmann and Amelung [16] (multi-layer model)	Lake Mead (filling)	leveling	2×10^{17}
Kaufmann and Amelung [16] (two-layer model)[c]	Lake Mead (filling)	leveling	1×10^{18}
Nishimura and Thatcher [134][d]	1959 Hebgen Lake eq.	leveling	4×10^{18}
Pollitz et al. [18][e]	1992 Landers eq.	GPS, InSAR	1–6×10^{18}
Pollitz [31][f]	1999 Hector Mine eq.	GPS	4.6×10^{18}
Lambeck et al. [129]	British Isles uplift (Holocene)	RSL(a)	3–6×10^{20}
Lambeck et al. [130][g]	Fennoscandia uplift (Holocene)	RSL(b)	4×10^{20}
Milne et al. [10]	Fennoscandia uplift (present)	GPS	5–10×10^{20}
Peltier [12]	global	RSL(b,c)	4×10^{20}
Mitrovica and Forte [135]	global	RSL(b,c) gravity	2×10^{21}
Kaufmann and Lambeck [14]	global	RSL(b,c), gravity, ER	5×10^{20}

Notes to Table 1:

[a] Viscosity of upper mantle at 125 km depth unless noted, published in last decade. All studies assume Maxwell viscoelastic rheology and multi-layer model with at least three layers (e.g., upper crust, lower crust, upper mantle) unless noted. Upper entries (above line) are western US, east of San Andreas fault and west of Colorado plateau; remaining entries represent GIA-based cratonic models or global models.

[b] Data: GPS = Global Positioning System; InSAR = Interferometric Synthetic Aperture Radar; RSL = Relative sea level curves from shoreline elevation data (a = British Isles; b = Fennoscandia, c = Hudson Bay); ER = Earth rotation.

[c] Valid for half space below 30 km depth.

[d] Valid for half space below 38 km depth.

[e] Valid for depth range 50–100 km.

[f] Steady state viscosity in linear biviscous model, valid below 30 km depth.

[g] Valid for depth range 150–200 km.

Pollitz at el. [18] infer a viscosity of 2.7×10^{18} Pa s beneath the Mojave Desert in the depth range 50–100 km based on GPS and INSAR observations of crustal deformation for 3 years following the 1992 Landers earthquake. The general similarity of these low viscosity western US estimates, despite significant differences in analytic technique, time scale, and nature of the loading phenomena, suggests that the contrast with GIA-based cratonic models is significant.

Models incorporating GIA data tend to have good depth resolution of upper mantle properties down to at least the 660–670 km discontinuity, but less resolution for lithospheric ($< \sim 100$ km) rheology due to the large diameter of the loads. In contrast, studies in the western US provide information on mantle properties shallower than ~ 150 km due to the local character of the loads (earthquakes; lake filling or drying). Subsequent figures and discussion include the depth range 50–150 km, although both classes of models only have common resolution in the depth range 100–150 km. Table 1 compares recent mantle viscosity estimates at 125 km depth for the two regions. The rheological contrast between them is actually more apparent in the depth range 50–100 km, immediately below the crust, but quantitative comparisons are difficult because of the aforementioned resolution issue. This depth range is generally considered lithospheric mantle in cratonic regions (with essentially infinite viscosity), whereas in the western US, most modern ($\sim$ last decade) geodetic studies resolve a very low viscosity uppermost mantle here, so low in fact that lithospheric mantle may be thin or even absent. These geodetic studies are in qualitative agreement with both seismic data [19,20] and dynamic elevation models based on gravity and topography data [21] that suggest a thin lithosphere through much of the western US. In this view, lithospheric strength here would reside mainly in the crust [22].

3. Non-linear rheology and effective viscosity: effects of strain rate, temperature, pressure, and water content

Most estimates for upper mantle viscosity are based on models that assume Maxwell rheology, with elastic solid behavior on short time scales, and Newtonian viscous fluid behavior (linear stress–strain rate relationship) on long time scales. The actual rheology of the upper mantle above ~ 200 km is probably better represented by thermally activated power law creep [23–25], as evidenced by seismic anisotropy in the upper mantle beneath oceans [26] and continents [27]. In this case, there is a non-linear relation between stress and strain rate. We can nevertheless define an effective viscosity at a given strain rate.

Large transient motions within a few months of major earthquakes can be interpreted in terms of extremely low viscosities for the uppermost mantle, perhaps reflecting this power law dependence and the influence of high stress–high strain rate conditions in the immediate post-seismic period [18,28,29]. These transients may also reflect the influence of afterslip and/or transient or bi-viscous rheology [30,31]. If we ignore these shortest term post-seismic transients and focus instead on responses over several years or longer, then a more coherent picture emerges, with a range of loading phenomena with greatly different time scales (several years to several thousand years) leading to broadly similar viscosity estimates. Thus, while strain rate certainly influences effective viscosity, strain rate differences alone are unlikely to be the primary explanation for the regional viscosity differences noted above.

Water dissolved in nominally anhydrous minerals such as olivine is now recognized as a ubiquitous component in the mantle [32,33]. Laboratory measurements indicate that olivine, the primary constituent of the upper mantle, is significantly weakened by the presence of water, lowering effective viscosity relative to dryer mantle at a given temperature and strain rate [34–39]. Regional and depth differences in the water concentration of the upper mantle can vary by more than one order of magnitude, and may therefore exert significant control on effective viscosity. For non-linear power law creep, the appropriate constitutive law for olivine in the shallow upper mantle, the relation between strain rate, stress, temperature and water fugacity is [37–39]:

$$\dot{\varepsilon} = A\sigma^n f_{H_2O}^r \exp^{-(H^*/RT)} \quad (1)$$

where $\dot{\varepsilon}$ is the strain rate, σ is the stress, n is the stress exponent (typically 3.0–3.5 for olivine), $f_{H_2}O$ is the water fugacity, r is the fugacity exponent, R is the gas constant, H^* is the activation enthalpy ($H^* = Q^* + PV^*$,

where Q^* and V^* are the activation energy and volume, respectively), P is pressure, T is absolute temperature, and n, A, Q^* and V^* are determined experimentally for a given material (Table 2). The fugacity dependence of (1) can also be expressed in terms of water concentration in olivine (Table 3) [40].

Newtonian (linear) viscosity, η, is defined as $\sigma/\dot{\varepsilon}$. For power law creep, where strain rate is a function of stress, we can define an effective viscosity, η_{eff}, in terms of either constant stress or constant strain rate. Since geodetic data provide information on strain rate, we define η_{eff} at a given strain rate:

$$\eta_{\mathrm{eff}} = \dot{\varepsilon}^{(1-n)/n} f_{\mathrm{H_2O}}^{-r/n} \left(A \exp^{-(H^*/RT)}\right)^{-1/n} \quad (2)$$

3.1. Strain rate

For the western US, surface strain rates near major active faults are of order 10^{-14} s^{-1} during the interseismic period. Strain rates through most of the Great Basin are lower, while strain rates in the immediate post-seismic period, and strain rates at depth within the actively deforming ductile mantle shear zone beneath crustal faults, may be higher. We considered a range of 10^{-13}–10^{-15} s^{-1} in the models presented below. For continental interiors rebounding after major deglaciation, strain rates as high as 10^{-15} s^{-1} may briefly characterize the period immediately after rapid glacier retreat, comparable to "background" strain rates associated with mantle convection (e.g., [41]). However, typical present-day strain rates associated with post-glacial rebound are probably lower (10^{-16}–10^{-17} s^{-1}). We considered a range of 10^{-15}–10^{-17} s^{-1}.

Table 2
Material constants

	A	Q^* (J/mol)	V^* (m^3/mol)
Dry dislocation	1.1×10^5 $(MPa)^{-n}/s$	5.30×10^5 (± 0.04)	20×10^{-6}
Wet dislocation (constant f_{H_2O})	1600 $(MPa)^{-(n+r)}/s$	5.20×10^5 (± 0.4)	22×10^{-6}
Wet dislocation (constant C_{OH})	90 $(MPa)^{-(n+r)}/s$	4.80×10^5 (± 0.4)	11×10^{-6}

n (stress exponent) = 3.5, r (fugacity exponent) = 1.2 for wet dislocations [40].

Table 3
Geotherms, solubility data for water in olivine, and sample viscosity calculation

Depth (km)	P[a] ($\times 10^9$ Pa)	T[b] (°C) WUS	T[c] (°C) Craton	f_{H_2O}[d] (MPa)	H_2O[e] ol.sat. (ppm)	C_{OH}[f] ol.sat. (H/10^6Si)
50	1.6	1100	520	7.20×10^3	84	1361
75	2.4	1200	670	2.07×10^4	130	2106
88	2.8	1265	754	3.79×10^4	177	2867
100	3.2	1300	819	6.41×10^4	240	3888
125	4.0	1350	942	1.83×10^5	350	5670
135	4.3	1372	1000	2.75×10^5	395	6399
150	4.8	1400	1085	5.46×10^5	468	7582

Sample calculation:

(1) Water-saturated, 125 km, T_{Vp} geotherm, strain rate 10^{-14} s^{-1}

$$\eta_{\mathrm{eff}} = \dot{\varepsilon}^{\left(\frac{1-n}{n}\right)} A^{\frac{-1}{n}} f_{\mathrm{H_2O}}^{\frac{-r}{n}} \left[\exp\left(-\frac{(H+PV)}{RT}\right)\right]^{\frac{-1}{n}} 10^6$$

$$\eta_{\mathrm{eff}} = (10^{-14})^{\left(\frac{1-3.5}{3.5}\right)} (1600)^{\frac{-1}{3.5}} (1.83 \times 10^5)^{\frac{-1.2}{3.5}} \times \left[\exp\left(-\frac{(520{,}000 + (4 \times 10^9)(22 \times 10^{-6}))}{(8.314)(1623)}\right)\right]^{\frac{-1}{3.5}} 10^6$$

$$\eta_{\mathrm{eff}} = 7.35 \times 10^{18} \text{ Pa–s}$$

(2) 50 ppm water in olivine, constant C_{OH}, 125 km, T_{Vp} geotherm, strain rate 10^{-14} s^{-1}:

$$\eta_{\mathrm{eff}} = \dot{\varepsilon}^{\left(\frac{1-n}{n}\right)} A^{\frac{-1}{n}} C_{\mathrm{OH}}^{\frac{-r}{n}} \left[\exp\left(-\frac{(H+PV)}{RT}\right)\right]^{\frac{-1}{n}} 10^6$$

$$\eta_{\mathrm{eff}} = (10^{-14})^{\left(\frac{1-3.5}{3.5}\right)} (90)^{\frac{-1}{3.5}} (810)^{\frac{-1.2}{3.5}} \times \left[\exp\left(-\frac{(480{,}000 + (4 \times 10^9)(11 \times 10^{-6}))}{(8.314)(1623)}\right)\right]^{\frac{-1}{3.5}} 10^6$$

$$\eta_{\mathrm{eff}} = 1.83 \times 10^{19} \text{ Pa–s}$$

[a] Assumed density of 3.2 g/cm^3.
[b] Mean geotherm for Western US from P-wave tomography [46].
[c] Mean geotherm for old continental lithosphere [44].
[d] Fugacity calculated from [136] at 1100 °C [49].
[e] Water solubility in olivine [49]. These values may be low by up to a factor of 3 [50].
[f] Calculated assuming water is distributed in nominally anhydrous minerals as discussed in [38]: mantle composed of 56% olivine, 19% opx, 10% cpx and 15% garnet and $D_{OH}^{Ol-Opx} = 0.2$, $D_{OH}^{Ol-Cpx} = 0.1$, and $D_{OH}^{Ol-Gt} = 1$.

3.2. Temperature, pressure and activation volume

Temperature is a primary control on effective viscosity. Much of the western US is characterized

by elevated heat flow, in the range 60–90 mW/m^2 (e.g., [42]) in contrast to Fennoscandia, Hudson Bay and other Precambrian shields with low heat flow, ~35–45 mW/m^2. Shield areas and active tectonic regions with surface heat flows of 40 and 75 mW/m^2, respectively, have temperature differences at 150 km depth of ~300–400 °C for standard conductive geothermal profiles (e.g., [43,44]). For cratonic areas, we use the "shield intraplate" geotherm of Green and Falloon [44]. For the western US, there may be significant spatial variation and hence uncertainty in the appropriate average geotherm. We considered four (Fig. 1): 1) the "young continental" geotherm of Green and Falloon [44]; 2) an average western US geotherm based on heat flow and heat production data [45]; 3 and 4) average western US geotherms based on P- and S-wave seismic tomography [46]. To address pressure effects, we use the activation volume estimates for olivine in Hirth and Kohlstedt [40] (Table 2).

3.3. Water

Under water-saturated conditions ("wet"), viscosities decrease with increasing pressure because (1) water fugacities increase strongly with pressure, (2) water solubility in olivine increases with increasing water fugacity (e.g., [47–49], and (3) viscosities decrease with increasing water concentrations (e.g., [39]). The saturation value of water in olivine at a given depth or pressure thus provides an upper limit to water concentration, and a lower limit for viscosity, at a given temperature and strain rate. Water solubility in olivine between 75 and 150 km depth is ~135 to 500 ppm [49]. Note that our "wet" values refer to water-saturated conditions, whereas Hirth and Kohlstedt [38] used "wet" to describe olivine with ~50 ppm water within a peridotitic mantle source containing ~125 ppm H_2O, appropriate for shallow mantle sources of mid-ocean ridge basalts. At a depth of 150 km, 50 ppm water in olivine represents roughly 10% of the saturation value (Table 3) and may be better referred to as "damp". Thus, water contents could be significantly higher, and viscosity significantly lower, than predicted by either dry or "damp" olivine values. However, most of the viscosity reduction in olivine occurs with the first ~50–100 ppm of H_2O.

A reevaluation of the calibration of the infrared spectroscopic technique used in recent solubility experiments (e.g., [49]) showed that actual water solubilities may be greater by up to a factor of 3 [50]. This would not affect viscosities calculated assuming water-saturated conditions, because a factor of 3 increase in water concentration would be balanced by a factor of 3 decrease in the pre-exponential constant A [40]; however, it does affect our interpretation of water concentrations as a function of pressure. We use the results of Kohlstedt et al. [49] and note that they may be low by up to a factor of 3.

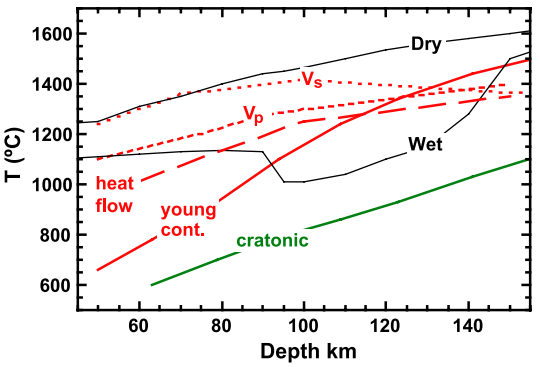

Fig. 1. Geotherms for continental shields (green) and western US (red) compared to upper mantle solidii (black) under dry and wet conditions. "Cratonic" is shield intraplate geotherm [44]. "Young Continental" is geotherm for continental area with moderately high heat flow [44]. "Heat Flow" is geotherm based on heat flow and heat production data for western US [45]. "V_p" and "V_s" are average geotherms based on P-wave and S-wave tomographic inversion for western US [46]. "Dry" is pyrolite (~upper mantle) solidus, "Wet" is solidus for pyrolite + fluid (C + H + O) [44].

4. Results

Fig. 2 compares estimated viscosities for cratonic areas based on GIA or global models and the western US based on geodesy to calculated effective viscosities for olivine, for water contents ranging from dry to fully saturated, using the solubility values of Kohlstedt et al. [49] and appropriate geotherms. For cratonic regions, good fits are obtained if olivine in the shallowest upper mantle (shallower than 80–120 km) is dry, while olivine at deeper levels is damp or

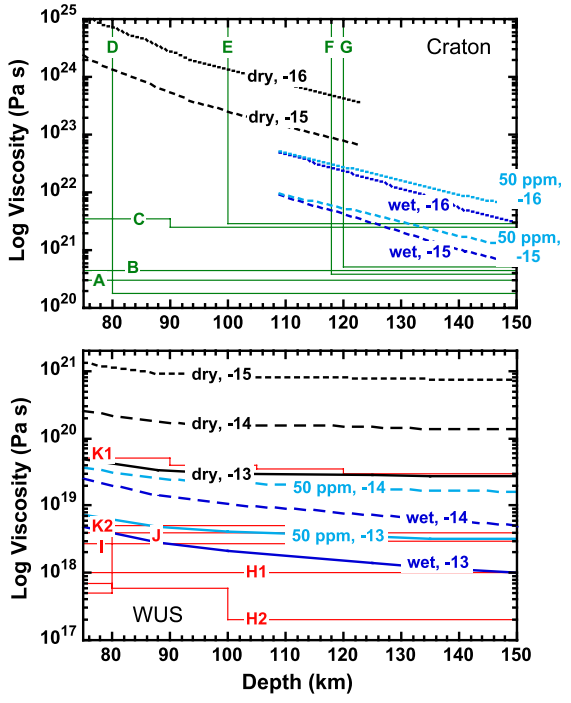

Fig. 2. Viscosity vs. depth for cratonic regions or global averages (top, green lines, A–G) and western US (bottom, red lines, H–K) compared to calculated values (Eq. (2), this study). Cratonic and global values from fig. 10 of Kaufmann and Lambeck [14], original sources below. A is [129]; B is [130]; C is [131]; D is [132]; E is [133]; F is [12]; G is [14]; H is [16] (H1 is 2 layer model, H2 is multi-layer inverse model, Fig. 14); I is [18], valid for depth range 50–100 km; J is [134]; K is [17] (K1 from Fig. 11, K2 from Fig. 12). Calculated viscosities (black or blue lines) use shield intraplate geotherm (top) [44] or average western US geotherm (T_{Vp}; base) [46]. Labels indicate water content (ppm by mass in olivine) and log. (base 10) of strain rate. "Wet" indicates water saturation.

wet. The damp and wet viscosity values are similar, differing by about a factor of 2 at 150 km depth.

For the western US, the Vp-based tomographic geotherm (hereafter T_{Vp} [46]) is used in subsequent figures and discussion. It provides a good fit to the viscosity data over the entire depth range, and predicts temperatures that are above the wet solidus for most of the depth range 50–150 km, but ~ 150–200 °C less than the dry solidus (Fig. 1). This latter point is important: geochemical and petrologic evidence to be discussed suggest high water concentrations in the western US upper mantle, and therefore appear to preclude temperatures as high as the dry peridotite solidus. At temperatures corresponding to a depth of 150 km, there is a factor of 30 difference in viscosity between dry and water-saturated olivine, of which a factor of 10 represents the difference between the dry and damp cases, and an additional factor of 3 represents the difference between the damp and wet cases (the differences increase with depth until the wet solidus is reached, because the solubility of water in olivine increases with pressure). Using T_{Vp}, the geodetically estimated viscosity profiles in the western US are best matched if olivine has high water contents, close to water-saturation, except for the very high strain rate case (10^{-13} s^{-1}), where olivine with 50 ppm water (damp) also provides a good fit. Since several of the geodetic studies reflect presumably slow mantle response to lake filling or drying, these high strain rates seem unlikely to us, suggesting that olivine over this depth range is water-saturated or nearly so. However, given uncertainties in the geodetic viscosity estimates and the experimental data, water concentrations of ~ 50 ppm or higher in olivine satisfy the available data.

5. Discussion

5.1. Why continental interiors are dry at depths shallower than 100–150 km

Because of differing geologic histories, the uppermost mantle beneath stable Precambrian shields and active tectonic regions like the western US have different compositions, especially with respect to water. Ancient shields in continental interiors have relatively dry, depleted uppermost mantle rocks that probably constitute a significant fraction of the ~ 50–150 km thick "lithosphere" defined in many earth rheological models. In this region, high degrees of melting that originally established melt-depleted, Mg-rich and Ca, Al, Fe-poor cratonic mantle [51,52] efficiently stripped incompatible elements, including water, from the upper mantle source, reflecting the high solubility of water in the melt compared to the solid fraction [53–56]. The subcratonic mantle root is an effective barrier to advective heat transfer, and its low temperatures trap inviscid, volatile-rich, low-melting point components over geologic time. Thus, metasomatic processes can cause net rehydration and re-enrichment of incompat-

ible elements, consistent with LREE-enriched trace element patterns in cratonic mantle garnets and pyroxenes, and the presence of small quantities of hydrous minerals, notably phlogopite. However, evidence from heat flow constraints [57] indicates that these metasomatic events do not pervade most cratonic uppermost mantle. In South Africa, where such metasomatism is well developed, Boyd et al. [58] note that most of the mantle lithosphere, from the base of the crust to a depth of 100 km or so, is relatively free of phlogopite. Typical water concentrations in olivine from South African garnet peridotites are near 70 ppm at 180 km depth where melt-related metasomatism is prominent, decreasing to 40–50 ppm at 130 km (D.R. Bell, unpublished data). Garnets within South African garnet peridotite contain less water than coexisting olivines [33,59,60], typically less than 50 ppm [59]. By inspection of Fig. 2, we can see that it is possible to construct a composite profile consistent with essentially all available geochemical and GIA data: e.g., at a strain rate of 10^{-16} s^{-1}, dry olivine to a depth of 120 km, and damp to wet olivine below 120 km.

In summary, most of the cold continental mantle root shallower than ~120 km is dry and strong, and likely to remain so for long periods of geologic time.

5.2. Western US upper mantle water contents

In contrast to cratonic areas, a variety of geochemical and petrologic data indicate that most of the uppermost mantle beneath the western US is anomalously wet. These data can be grouped into four classes. First, the presence of hydrous minerals in otherwise normal mantle assemblages implies wetter than normal conditions (typical mantle lacks hydrous phases). A number of petrological studies document unusually abundant hydrous phases in Colorado Plateau mantle xenoliths, including humite group minerals, serpentine, chlorite, and amphibole [61–70]. Post-10 Ma basaltic lavas erupted in the Rio Grande Rift and Basin and Range commonly contain amphibole megacrysts derived from the mantle [71]. Best [72,73] and Matson et al. [74] described Holocene–Recent basanites in the Grand Canyon area of Arizona with mantle-derived inclusions containing amphibole. Bergman et al. [75] described an amphibole-bearing peridotite nodule in basanite from Lunar Crater volcanic field, Nevada, which has eruptions from Late Pliocene to Holocene in age. Righter and Carmichael [76] demonstrate that amphiboles at Lunar Crater and other localities in the western US are true mantle samples and cannot have grown at a late stage in the basalt host, e.g., through later assimilation of hydrous crust.

Second, nominally anhydrous minerals in garnet peridotitic xenoliths in the western US are anomalously wet compared to those in cratonic garnet peridotites. For example, garnets from the mantle beneath the Colorado Plateau have much higher water contents than those of comparable cratonic mantle rocks. Garnets from both peridotites and eclogites of the Colorado Plateau commonly contain OH concentrations about 10 times the typical values from equivalent mantle rock types below the Siberian craton and the Kaapvaal craton of southern Africa [77–81].

Third, young basalts (generally alkalic) derived from western US mantle are anomalously wet, consistent with derivation from a wet mantle source. While this is usually difficult to observe (surface-erupted lavas are degassed), melt inclusions trapped in olivine phenocrysts in such lavas may retain evidence of original magmatic water contents. Fig. 3 shows data from well-preserved melt inclusions in Late Quaternary basalts from Yucca Mountain, Nevada [82] clearly showing high water characteristics, well in excess of typical MORB values. Hill et al. [83] discuss the presence of amphibole and the high water contents of these and related basalts, pointing out that they require 2 to 5 wt.% water in the original magma, implying (for 5% partial melting) a minimum of 1000 ppm water in the mantle source. For comparison, typical MORB sources contain ~50 (depleted) to 450 (enriched) ppm H_2O (e.g., [53]).

Fourth, other geochemical characteristics of post-20 Ma lavas are consistent with derivation from anomalously wet mantle. Whitlock [84] shows that post-mid Miocene (<14 Ma) basalts and basaltic andesites in northern California have chemical characteristics consistent with derivation from previously hydrated mantle wedge material which upwells into the slab window after passage of the Mendocino triple junction [85]. Lange et al. [86] describe 2–4 Ma mafic-intermediate lavas in the Mono Basin–

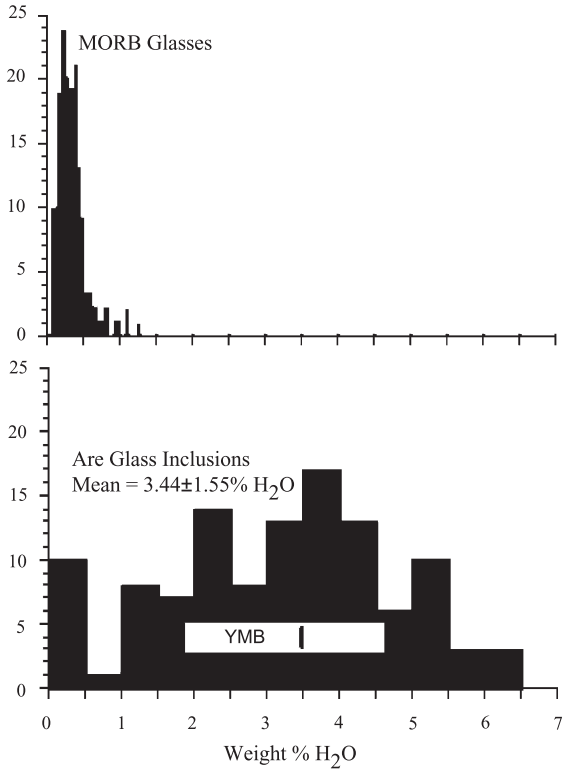

Fig. 3. Histograms showing water concentrations in MORB glasses (quenched under pressure) compared to glass inclusions in olivine phenocrysts (which may retain original water) from island arc basalts, modified from Stern [109]. White horizontal rectangle in island arc histogram (YMB) shows range of water in glass inclusions in basalts from Yucca Mountain, Nevada [82]. Vertical bar in white rectangle shows mean concentration for YMB (3.5%), similar to island arc mean (3.44%).

Long Valley area that record high water fugacity in the source region. Feldstein and Lange [87] document Late Pliocene lavas throughout the Sierra Nevada with high (>2 wt.%) pre-eruptive water contents.

The high water contents that we infer for the western US upper mantle suggest that dry melting models for this region (e.g., [88]) should be re-evaluated, for example using the new wet melting model of Asimow et al. [89].

5.3. Why the west is wet

We suggest that Farallon plate subduction plays a key role in explaining anomalously low viscosity in the western US upper mantle, through its influence on water contents [90]. In contrast to cratonic regions, which have been stable for time scales of order 10^9 years, most of western North America experienced a long (>100 million year) period of subduction in Mesozoic and Cenozoic time, ending ~30 Ma [91]. Subduction cools and hydrates the upper mantle above the downgoing plate, as hydrothermally altered oceanic crust and water-saturated sediment undergo dehydration and metamorphism, forcing water out of the subducting plate and into the overlying mantle wedge (e.g., [92,93]). Studies of water concentrations in arc and back-arc lavas (e.g., [94,95] and in corresponding melt inclusions in phenocrysts (e.g., [96]) confirm that the source region for arc lavas (~100 km depth) is anomalously wet (~250 to 2500 ppm H_2O) compared to mantle sources for MORB (~50–450 ppm H_2O [33,53,96–100] and OIB (~400 to 1000 ppm H_2O [89,100–105]). Parts of this source region almost certainly have water contents well in excess of olivine solubility, as evidenced by the presence of hydrous phases such as serpentine (e.g., [105,106]).

The amount of residual water that survives the "subduction gauntlet" and is retained in the downgoing slab to enter the deep mantle has until recently been quite uncertain. However, new work suggests that such retained water is negligible, implying that large amounts of subducted water are available to hydrate the upper mantle. Measurements of volatile contents of plume-generated ocean island basalts show that plumes containing components of previously subducted lithosphere are relatively dry compared to other mantle sources, indicating that water is efficiently extracted during the subduction process [107,108]. Thus, water in the subducted slab must be either expelled through fluid venting in the fore-arc, expelled during island arc magmatic processes, or sequestered in the overlying mantle wedge. Water initially expelled at shallow mantle levels may be entrained in the boundary zone between the downgoing slab and the overlying mantle due to viscous drag, and dragged to somewhat deeper levels [109]. Seismic tomography suggests that large volumes of mantle above long-lived subduction zones are anomalously wet [110] perhaps down to depths of ~400 km [111].

Geochemical data support the idea that elevated water in western US amphibole megacrysts derives

from a subduction zone setting, even though the ages of these rocks are much younger than the end of Farallon plate subduction (~ 30 Ma). Samples not disturbed by surface fractionation effects are relatively rich in deuterium [112,113], consistent with derivation from dehydration of a subducted slab. Similar occurrences of hydrous phases and heavy D/H ratios are seen in other fossil subduction regions, such as the Eifel [114,115], and in active subduction regions such as Japan [116].

Usui et al. [117] demonstrate that eclogite xenoliths in Colorado Plateau magmatic bodies emplaced at 26–35 Ma contain low temperature/high pressure minerals, consistent with a subduction origin, and have ages in the range 33–81 Ma, consistent with derivation from the subducted Farallon plate. Smith [68,69] argued that hydration of the Colorado Plateau mantle occurred within 20 million years prior to transport of xenoliths in the 25–30 Ma eruptions of the Navajo Volcanic Field. This is consistent with the idea that mantle hydration occurred sometime during the long period of flat slab subduction of the Farallon plate beneath North America, ~ 80–30 Ma (e.g., [90,118–120]), and occurred well inland of the coastal region. During flat slab subduction, the zone of maximum slab dehydration (and the corresponding zone of upper mantle hydration above it) presumably moved inland. Most of the original lithospheric mantle beneath the western US probably experienced significant hydration above ~ 150 km depth, except where slab dip eventually steepened, beneath the Colorado Plateau, where deeper hydration likely occurred. Although initially cooled by the presence of a relatively cold slab, this hydrated lithospheric mantle began to warm at the end of flat slab subduction, gradually attaining its current hot, wet, low viscosity state. In effect, the low angle Farallon slab advected water hundreds of km northeast of the coastal region, as the hinge zone migrated east, eventually hydrating a huge volume of upper mantle, not just a narrow mantle wedge near the active coastal arc.

A key question is whether western North America's upper mantle could retain significant water 20–30 million years after subduction stopped. A period of extensive Miocene (~ 10–20 Ma) magmatic activity throughout the western US occurred shortly after the end of flat slab subduction and is thought to represent the replacement of cold subducted slab as hot asthenosphere upwelled into the slab window. Could this activity have "cleansed" the upper mantle of its high water content? The best evidence against this is the fact that indicators of anomalously wet mantle include products that are much younger than 10 Ma, including Holocene lavas and young lavas hosting wet xenoliths. Several studies have noted the large time lags that are possible between subduction-related hydration and later eruption of hydration-influenced volcanics (e.g., [86,87]).

Removal of water from the mantle requires elevation of mantle temperatures above dehydration reactions (~ 1100 °C for amphibole, the most thermally stable mineral) and melting to extract water bound in nominally anhydrous minerals. If hydrous phases are present in sufficiently large concentration, the mantle is effectively buffered for a considerable period of time. This suggests that thorough dehydration requires major tectono-thermal processing and melting of the mantle. In the absence of large-scale mantle overturn this may take tens to hundreds of millions of years. If this scenario is correct, most of the present-day upper mantle beneath the western US is still significantly wetter than the relatively dry, depleted uppermost mantle beneath cratons, although the pulse of post-20 Ma volcanism in the western US presumably represents the beginning of large scale tectono-thermal processing of this region, as the hydrous mantle warms and begins to melt.

Even if convection has succeeded in mixing or replacing some or most of the original hydrated mantle in the western US in the last 20 million years, replacement mantle (upwelling asthenosphere, whether typical MORB or enriched OIB mantle) is still likely to be significantly wetter than typical lithospheric mantle beneath cratons (Table 4). Thus, another scenario consistent with available data is that the locations of hydrous phases and wet basalts in the western US are not reflective of average mantle conditions here, but rather indicate anomalously enriched mantle pods ("plum pudding" model). The generally low viscosity of the region would then reflect the influence of upwelling asthenosphere combined with the lack of typical cratonic lithospheric mantle. In this scenario, the main role of Farallon plate subduction is to thin or remove the initially strong, dry uppermost mantle in the western US, by hydrating and weakening it, perhaps facilitating de-

Table 4
Water concentrations in mantle source regions

Environment	Magma wt.% H_2O	Lherzolite wt.% H_2O	Olivine ppm H_2O[a]	Olivine 10^3 H/10^6Si	Sat at 120 km?
MORB[b]	0.1	0.012	50	0.8	no
EMORB and OIB[c]	0.3–1.0	0.03–0.08	125–330	2.0–5.3	no
BABB[d]	0.2–2.0	0.024–0.50	100–2000	1.6–32	maybe
Arc[e]	2.0–8.0	0.25 to 1	1000–?[f]	1.6–?[f]	maybe

Concentrations of water in magmas and mantle source regions from:

[a] Values calculated as in [38] assuming a garnet pyrolite assemblage of 56% olivine, 19% opx, 10% cpx and 15% garnet and olivine–mineral partition coefficients for water of 0.2 for olivine-opx, 0.1 for olivine-cpx, and 1 for olivine–garnet.

[b] [54,96,97,99].

[c] [100–102,104,107].

[d] [94,95,137].

[e] [138–140].

[f] Water concentration in olivine uncertain due to probable presence of hydrous phases.

lamination and allowing replacement asthenosphere to upwell essentially to the base of the crust.

5.4. Seismic tomography

Seismic tomography is achieving sufficient resolution to probe the characteristics of the upper mantle with increasing detail. In the western US, slow seismic velocity anomalies in the upper mantle have long been recognized (e.g., [121–123]) and are often interpreted in terms of relatively hot, dry mantle. However, high water concentrations may also reduce seismic velocities [124].

The presence of water potentially affects seismic velocities in at least five ways:

1. It promotes melting by lowering the solidus temperature of the mantle;
2. It may lead to the presence of a hydrous fluid;
3. It promotes the development of hydrous minerals such as amphibole and phlogopite, which are seismically slower than olivine;
4. It increases the water concentration in nominally anhydrous minerals such as olivine, increasing anelasticity and hence attenuation [124];
5. It changes the anisotropy of the mantle [125].

Items (1) and (2) may be relatively minor effects, because the extremely low viscosity of melts and hydrous fluids at high temperatures means that these low density liquids rapidly migrate away (up) from the source. Karato [124] suggests that on geologic time scales, it is unlikely that melt exceeds 1% by volume through most of the upper mantle due to this effect, and hence would have a negligible effect on seismic velocity. In the event of significant partial melting, high melt concentrations will accumulate at density discontinuities such as the crust–mantle boundary, intrude the crust, or erupt as volcanoes. Depending on depth resolution, such melt concentrations could affect tomographic results near the crust–mantle boundary (30–50 km), but perhaps are less important for deeper regions.

Water in the upper mantle affects both Vs and Vp, but we are not aware of quantitative studies that address covariation of seismic velocity with temperature, water content in olivine, presence of hydrous phases, and partial melt. Goes and van der Lee [46] invert seismic velocity data for temperature in the North American upper mantle and compare these estimates to independent data. They note that the Cascadia upper mantle, expected to be water-rich due to present-day subduction, has the slowest Vs anomaly in the western US (model NA00) and discrepant Vp versus Vs temperature estimates, with Vs-based temperature (T_{Vs}) much higher than Vp-based temperature (T_{Vp}) in the depth range 50–150 km (their Fig. 7). Assuming that this discrepancy is characteristic of strongly hydrated mantle (for any or all of the five reasons listed above) we can investigate hydration effects in the tomographic results for other regions. T_{Vs} and T_{Vp} estimated by Goes and van der Lee [46] for most parts of the eastern US agree quite well, consistent with our hypothesis of a relatively dry cratonic upper mantle. However, much of the western US exhibits T_{Vp} versus T_{Vs} discrepancies in the depth range 50–110 km, in the sense expected for

hydration (T_{Vs}>T_{Vp}; Figs. 3 and 5 of Goes and van der Lee [46]. In particular, the Basin and Range and Colorado Plateau both exhibit T_{Vs}>T_{Vp}, and T_{Vs} above the dry peridotite solidus in some areas, in the depth range where geochemical data require high water contents; both regions were affected by flat slab subduction (Fig. 4). For example, the eastern Colorado Plateau and southern Rocky Mountains both have large areas where T_{Vs} exceed 1500 °C at 110 km depth, at or above the dry peridotite solidus (Fig. 1) and several hundred degrees higher than T_{Vp}, suggesting that T_{Vs} is too high, and T_{Vp} is a more reliable temperature estimate. The 1100 °C "isotherm" defined by T_{Vs} approximately matches the maximum inland penetration of the Farallon slab (Fig. 4), consistent with the idea that this may define a hydration front rather than a true temperature line.

The geodetic viscosity estimates for the western US have little resolution beyond 150 km, but the depth extent of hydration can also be addressed (at least qualitatively) with the tomographic data. $T_{Vs} \sim T_{Vp}$ below 150 km in the results of Goes and van der Lee [46] suggesting that anomalously high water concentrations are restricted to depths shallower than 150 km. This is also the depth where T_{Vp} crosses the wet peridotite solidus (Fig. 1), suggesting that differences between T_{Vs} and T_{Vp} in the uppermost mantle may reflect the presence of small amounts of melt or

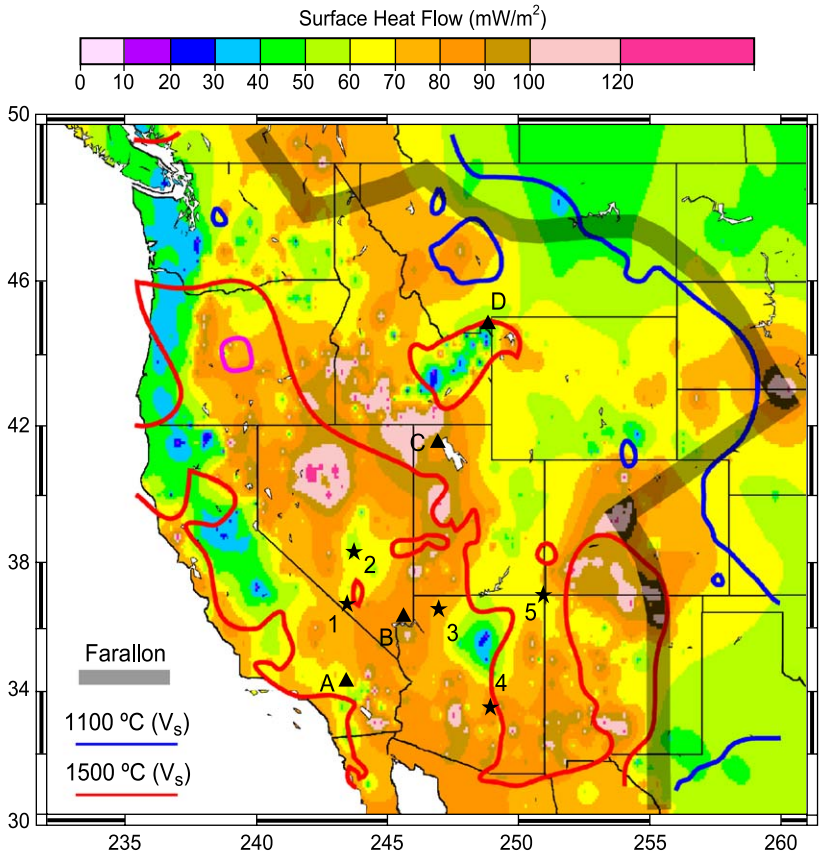

Fig. 4. Heat flow in the western US, compared to regions at 110 km depth where temperature estimates based on S-wave seismic tomography (T_{Vs} [46]) exceed 1100 °C (southwest of dark blue line) and 1500 °C (within red line), the approximate dry peridotite solidus at this depth. Dark grey band shows maximum extent of Farallon plate during flat slab subduction, modified from Bird [119] (note similarity to 1100 °C T_{Vs} isotherm). Stars with numbers show location of geochemical or petrologic indicators of hydrated upper mantle, which include regions of T_{Vs} above 1500 °C (1 is [72,73]; 2 is [141]; 3 is [75,76]; 4 is [76]; 5 is [117]). Triangles with letters show location of viscosity estimates discussed in text and Table 1 (A is [18,31]; B is [16]; C is [17]; D is [134]).

hydrous fluid. However, assessing the influence of such fluids on overall viscosity and the passage of seismic waves is not straightforward. For example, small amounts of melt could increase seismic attenuation and decrease effective viscosity, for example by enhancing grain boundary sliding. On the other hand, water is partitioned strongly into melt, hence water concentration in olivine would decrease, raising its effective viscosity.

In summary, upper mantle viscosity estimates in the western US ($\sim 10^{18}$ Pa s) are characteristic of hot, wet mantle, and are lower than the viscosity of cool, wet upper mantle in modern subduction zones ($\sim 10^{19}$ Pa s), for example observed in the modern Cascadia arc on the basis of relative sea level data [126]. Both values are lower than typical cratonic values, with cool, damp to wet asthenosphere at low strain rates (10^{20}–10^{21} Pa s) deeper than about 120 km depth, or cool, dry lithosphere at shallower levels, with much higher or essentially infinite viscosity.

5.5. Plate dynamics, the Wilson cycle, long-lived plate boundary zones and strength of the upper mantle

Subduction of cold oceanic lithosphere cools the surrounding mantle, raising viscosity and increasing drag on the down-going plate. However, water released by the downgoing slab counteracts this effect, weakening the surrounding mantle and making it easier to sustain subduction [127]. Long-lived subduction margins will accumulate large amounts of water in the upper mantle, and may therefore stay weak for tens and possibly hundreds of millions of years after subduction stops. Future plate boundaries will therefore tend to occur in the same place, exploiting the previously weakened region, perhaps explaining the tendency for repeated opening and closing of ocean basins along the same plate boundary zone (Wilson cycle).

The western US has long been recognized as a unique tectonic environment, with diffuse deformation and magmatism occurring many hundreds of km inland from the main plate boundary, the San Andreas fault. The diffuse nature of present-day deformation here may reflect the presence of anomalously weak upper mantle over a broad region, in turn reflecting the history of flat slab subduction and consequent hydration of large volumes of upper mantle as far inland as the Colorado Plateau. With passage of the Farallon plate, the newly hydrated, cool upper mantle was exposed to warmer mantle below the slab [90]. As the hydrated material warmed, it attained anomalously low viscosity, becoming highly mobile, capable of rapid, small scale convection, promoting magmatic activity [85,128].

Maggi et al. [22] used earthquake focal depths to suggest that the upper mantle beneath continents in general has relatively little strength, which they suggest reflects the presence of water. We have emphasized the importance of lateral heterogeneity in mantle properties and hence would put a more nuanced interpretation on their observations. The earthquakes used by Maggi et al. [22] invariably occur in or near active tectonic regions (plate boundary zones), marginal to cratonic areas. Most of these regions were also subject to past subduction-related hydration (e.g., Zagros, Aegean), as in our western US example. We suggest that these regions are weak, not because they are typical continental regions, but because they are atypical, with a history of subduction at or near the margins of larger cratonic areas. In our model, interior cratonic regions retain a strong (cold, dry) lithospheric upper mantle, and generally remain immune to tectonic disruption, even in the presence of multiple Wilson cycles.

Acknowledgements

We thank Bob Stern and Saskia Goes for providing data and digital versions of several figures, and Britt Hill, David Kohlstedt, Sash Majumder, Ted Scott and Francis Albarede for discussion and comments. Reviews by Fred Pollitz, Gene Humphreys and Greg Hirth greatly improved the paper. This work was supported by grants from NSF, NASA and ONR. ***[SK]***

References

[1] C.F. Yoder, J.G. Williams, J.O. Dickey, B.E. Schutz, R.J. Eanes, B.D. Tapley, Secular variation of the Earth's gravitational harmonic J2 coefficient from LAGEOS and nontidal acceleration of Earth rotation, Nature 303 (1983) 757–762.

[2] E.R. Stephenson, L.V. Morrison, Long term fluctuations in the Earth's rotation: 700 B.C. to A.D. 1990, Philos. Trans. R.

Soc. Lond., Ser. A 351 (1995) 165–202, Trans. R. Soc. London, Ser. A 334 (1978) 110–125.
[3] R. Sabadini, D.A. Yuen, E. Boschi, Polar wander and the forced responses of a rotating, multilayered, viscoelastic planet, J. Geophys. Res. 87 (1982) 2885–2903.
[4] W.E. Carter, D.S. Robertson, T.E. Pyle, J. Diamante, The application of geodetic radio interferometric surveying to the monitoring of sea level, Geophys. J. R. Astron. Soc. 87 (1986) 3–13.
[5] G. Spada, Y. Ricard, R. Sabadini, True polar wander for a dynamic Earth, Nature 360 (1992) 452–454.
[6] L.M. Cathles, The Viscosity of the Earth's Mantle, Princeton Univ. Press, Princeton, NJ, 1975.
[7] W.R. Peltier, W.E. Farrell, J.A. Clark, Glacial isostasy and relative sea level: a global finite element model, Tectonophysics 50 (1978) 81–110.
[8] A.M. Tushingham, W.R. Peltier, Validation of the ICE-3G model of Würm-Wisconsin deglaciation using a global data base of relative sea level histories, J. Geophys. Res. 97 (1992) 3285–3304.
[9] D.F. Argus, Postglacial rebound from VLBI geodesy: on establishing vertical reference, Geophys. Res. Lett. 23 (1996) 973–976.
[10] G.A. Milne, J.L. Davis, J.X. Mitrovica, H.-G. Scherneck, J.M. Johansson, M. Vermeer, H. Koivula, Space-geodetic constraints on glacial isostatic adjustment in Fennoscandia, Science 291 (2001) 2381–2385.
[11] K.D. Park, R.S. Nerem, J.L. Davis, M.S. Schenewerk, G.A. Milne, J.X. Mitrovica, Investigation of glacial isostatic adjustment in the northeast US using GPS measurements, Geophys. Res. Lett. 29 (2002) (10.1029/2001GLO13782).
[12] W.R. Peltier, Post-glacial variations in the level of the sea: implications for climate dynamics and solid earth geophysics, Rev. Geophys. 36 (1998) 603–689.
[13] K. Lambeck, P. Johnston, The viscosity of the mantle: evidence from analyses of glacial rebound phenomenon, in: I. Jackson (Ed.), The Earth's Mantle: Composition, Structure and Evolution, Cambridge Univ. Press, Cambridge, UK, 1998, pp. 461–525.
[14] G. Kaufmann, K. Lambeck, Glacial isostatic adjustment and the radial viscosity profile from inverse modeling, J. Geophys. Res. 107 (2002) 2280(10.1029/2001JB000941).
[15] W.P. Peltier, Global glacial isostatic adjustment and modern instrumental records of relative sea level history, Sea level rise; history and consequences, Int. Geophys. Ser. 75 (2001) 65–95.
[16] G. Kaufmann, F. Amelung, Reservoir-induced deformation and continental rheology in vicinity of Lake Mead, Nevada, J. Geophys. Res. 105 (2000) 16341–16358.
[17] B.G. Bills, D.R. Currey, G.A. Marshall, Viscosity estimates for the crust and upper mantle from patterns of lacustrine shoreline deformation in the eastern Great Basin, J. Geophys. Res. 99 (1994) 22059–22096.
[18] F.F. Pollitz, G. Peltzer, R. Bürgmann, Mobility of continental mantle; evidence from postseismic geodetic observations following the 1992 Landers earthquake, J. Geophys. Res. 105 (2000) 8035–8054.
[19] G. Zandt, S.C. Myers, T.C. Wallace, Crust and mantle structure across the Basin and Range–Colorado Plateau boundary at 37°N latitude and implications for Cenozoic extensional mechanism, J. Geophys. Res. 100 (1995) 10529–10548.
[20] L.A. Lastowka, A.F. Sheehan, J.M. Schneider, Seismic evidence for partial lithospheric delamination model of Colorado Plateau uplift, Geophys. Res. Lett. 28 (2001) 1319–1322.
[21] A.R. Lowry, N.M. Ribe, R.B. Smith, Dynamic elevation of the Cordillera, western United States, J. Geophys. Res. 105 (2000) 23371–23940.
[22] A. Maggi, J.A. Jackson, D. McKenzie, K. Priestly, Earthquake focal depths, effective elastic thickness, and the strength of the continental lithosphere, Geology 28 (2000) 495–498.
[23] A. Nicolas, N.I. Christensen, Formation of anisotropy in upper mantle peridotites: a review, in: K. Fuchs, C. Froidevaux (Eds.), Composition, Structure and Dynamics of the Lithosphere–Asthenosphere System, AGU Geodyn. Ser., vol. 16, 1987 pp. 111–124.
[24] S. Karato, On the Lehman discontinuity, Geophys. Res. Lett. 19 (1992) 2255–2258.
[25] S. Karato, P. Wu, Rheology of the upper mantle: a synthesis, Science 260 (1993) 771–778.
[26] C.E. Nishamura, D.W. Forsyth, The anisotropic structure of the upper mantle in the Pacific, Geophys. J. 96 (1989) 203–229.
[27] J.B. Gaherty, T.H. Jordan, Lehman discontinuity as the base of an anistropic layer beneath continents, Science 268 (1995) 1468–1471.
[28] T.-T. Yu, J.B. Rundle, J. Fernandez, Surface deformation due to a strike–slip fault in elastic gravitational layer overlying a viscoelastic gravitational half-space, J. Geophys. Res. 101 (1996) 3199–3214.
[29] F.F. Pollitz, C. Wicks, W. Thatcher, Mantle flow beneath a continental strike–slip fault: Postseismic deformation after the 1999 Hector Mine earthquake, Science 293 (2001) 1814–1818.
[30] E.R. Ivins, Transient creep of a composite lower crust: 2. A polymineralic basis for rapidly evolving post-seismic deformation modes, J. Geophys. Res. 101 (1996) 28005–28028.
[31] F.F. Pollitz, Transient rheology of the uppermost mantle beneath the Mojave Desert, California, Earth Planet. Sci. Lett. 215 (2003) 89–104.
[32] J.R. Smyth, D.R. Bell, G.R. Rossman, Incorporation of hydroxyl in upper-mantle clinopyroxenes, Nature 351 (1991) 732–735.
[33] D.R. Bell, G.R. Rossman, Water in the earth's mantle: the role of nominally anhydrous minerals, Science 255 (1992) 1391–1397.
[34] P.N. Chopra, M.S. Paterson, The role of water in the deformation of olivine, J. Geophys. Res. 89 (1984) 7861–7876.
[35] S.J. Mackwell, D.L. Kohlstedt, M.S. Paterson, The role of water in the deformation of olivine single crystals, J. Geophys. Res. 90 (1985) 11319–11333.
[36] S. Karato, M.S. Paterson, J.D. Fitzgerald, Rheology of synthetic olivine aggregates; influence of grain size and water, J. Geophys. Res. 91 (1986) 8151–8176.

[37] D.L. Kohlstedt, B. Evans, S.J. Mackwell, Strength of the lithosphere: constraints imposed by laboratory experiments, J. Geophys. Res. 100 (1995) 17587–17602.
[38] G. Hirth, D.L. Kohlstedt, Water in the oceanic upper mantle: implications for rheology, melt extraction and the evolution of the lithosphere, Earth Planet. Sci. Lett. 144 (1996) 93–108.
[39] S. Mei, D.L. Kohlstedt, Influence of water on plastic deformation of olivine aggregates 2: dislocation creep regime, J. Geophys. Res. 105 (2000) 21471–21481.
[40] G. Hirth, D.L. Kohlstedt, Rheology of the upper mantle and the mantle wedge: a view from the experimentalists, in: J. Eiler (Ed.), Inside the Subduction Factory, Am. Geophys. Union, Geophys. Monogr. Ser. 118 (2004) 83–106.
[41] D.L. Turcotte, G. Schubert, Geodynamics: Applications of Continuum Physics to Geological Problems, Wiley, New York, 1982, 450 pp.
[42] J.H. Sass, A.H. Lachenbruch, S.P. Galanis, P. Morgan, S.S. Priest, T.H. Moses, R.J. Munroe, Thermal regime of the southern Basin and Range province: 1. heat flow data from Arizona and the Mojave Desert of California and Nevada, J. Geophys. Res. 99 (1994) 22093–22119.
[43] G. Ranalli, Rheology of the Earth, 2nd ed., Chapman & Hall, London, 1995, 413 pp.
[44] D.H. Green, T.J. Falloon, Pyrolite: a Ringwood concept and its current expression, in: I. Jackson (Ed.), The Earth's Mantle: Composition, Structure and Evolution, Cambridge Univ. Press, Cambridge, UK, 1998, pp. 311–378.
[45] I.M. Artemieva, W.D. Mooney, Thermal thickness and evolution of Precambrian lithosphere: a global study, J. Geophys. Res. 106 (2001) 16387–16414.
[46] S. Goes, S. van der Lee, Thermal structure of the North American uppermost mantle inferred from seismic tomography, J. Geophys. Res. 107 (B3) (10.129, /2000JB000049).
[47] Q. Bai, D.L. Kohlsted, Substantial hydrogen solubility in olivine and implications for water storage in the mantle, Nature 357 (1992) 672–674.
[48] Q. Bai, D.L. Kohlstedt, Effects of chemical environment on the solubility and incorporation mechanism for hydrogen in olivine, Phys. Chem. Miner. 19 (1993) 460–471.
[49] D.L. Kohlstedt, H. Keppler, D.C. Rubie, Solubility of water in the a, b, and g phases of $(Mg,Fe)_2SiO_4$, Contrib. Mineral. Petrol. 123 (1996) 345–357.
[50] D.R. Bell, G.R. Rossman, J. Maldener, D. Endisch, F. Rauch, Hydroxide in olivine: a quantitative determination of the absolute amount and calibration of the IR spectrum, J. Geophys. Res. 108 (2003) doi:10.1029/2001JB000679.
[51] F.R. Boyd, S.A. Mertzman, Composition and structure of the Kaapvaal lithosphere, in: B.O. Mysen (Ed.), Magmatic Processes: Physicochemical Principles, Spec. Publ. - Geochem. Soc., 1987, pp. 13–24.
[52] F.R. Boyd, Compositional distinction between oceanic and cratonic lithosphere, Earth Planet. Sci. Lett. 96 (1989) 15–26.
[53] J.E. Dixon, E. Stolper, J.R. Delaney, Infrared spectroscopic measurements of CO_2 and H_2O in Juan de Fuca Ridge basaltic glasses, Earth Planet. Sci. Lett. 90 (1988) 87–104.
[54] P. Michael, Regionally distinctive sources of depleted MORB: evidence from trace elements and H_2O, Earth Planet. Sci. Lett. 131 (1995) 310–320.
[55] L.V. Danyushevsky, S.M. Eggins, T.J. Falloon, D.M. Christie, H_2O abundance in depleted to moderately enriched mid-ocean ridge magma, Pt. 1: incompatible behaviour, implications for mantle storage, and origins of regional variations, J. Petrol. 41 (2000) 1329–1364.
[56] C. Aubaud, E.H. Hauri, M.M. Hirschmann, Water partition coefficients between nominally anhydrous minerals and basaltic melts, Goldschmidt Geochemistry Conf., Abstract, vol. 559, 2004, Copenhagen.
[57] R.L. Rudnick, W.F. McDonough, R.J. O'Connell, Thermal structure, thickness and composition of continental lithosphere, Chem. Geol. 145 (1998) 395–411.
[58] F.R. Boyd, D.G. Pearson, S.A. Mertzman, Spinel facies peridotites from the Kaapvaal root, in: J.J. Gurney, et al. (Ed.), The J.B. Dawson Volume. Proc. 7th Int. Kimberlite Conference, vol. 1, Red Roof Design, Cape Town, 1999, pp. 40–48.
[59] D.R. Bell, G.R. Rossman, The distribution of hydroxyl in garnets from the subcontinental mantle of southern Africa, Contrib. Mineral. Petrol. 111 (1992) 161–178.
[60] D.R. Bell, G.R. Rossman, R.O. Moore, Abundance and partitioning of OH in a high-pressure magmatic system: megacrysts from the Monastery kimberlite, South Africa, J. Petrol., (2004) (in press).
[61] T.R. McGetchin, L.T. Silver, A.A. Chodos, Titanoclinohumite: a possible mineralogical site for water in the upper mantle, J. Geophys. Res. 75 (1970) 255–259.
[62] H.H. Helmstaedt, R. Doig, Eclogite nodules from kimberlite pipes of the Colorado Plateau—samples of subducted Franciscan-type oceanic lithosphere, Phys. Chem. Earth 9 (1975) 95–111.
[63] K. Aoki, K. Fujino, M. Akaogi, Titanochondrodite and titanoclinohumite derived from the upper mantle in the Buell Park kimberlite, Arizona, USA, Contrib. Mineral. Petrol. 56 (1976) 243–253.
[64] D. Smith, S. Levy, Petrology of the Green Knobs diatreme and implications for the upper mantle beneath the Colorado Plateau, Earth Planet. Sci. Lett. 29 (1976) 107–125.
[65] H.H. Helmstaedt, D.J. Schulze, Garnet clinopyroxenite–chlorite ecoplite transition in a xenolith from Moses Rock: further evidence for metamorphosed ophiolites under the Colorado Plateau, in: F.R. Boyd, H.O.A. Meyer (Eds.), The Mantle Sample: Inclusions in Kimberlites and Other Volcanics, AGU, Washington, 1979, pp. 357–365.
[66] H.H. Helmstaedt, D.J. Schulze, Eclogite-facies ultramafic xenoliths from Colorado Plateau diatreme breccias: comparison with eclogites in crustal environments, evaluation of the subduction hypothesis, and implications for eclogite xenoliths from diamondiferous kimberlites, in: D.C. Smith (Ed.), Eclogites and Eclogite Facies Rocks, Elsevier, New York, 1988, pp. 387–450.
[67] D. Smith, Hydrous minerals and carbonates in peridotite inclusions from the Green Knobs and Buell Park kimberlitic diatremes on the Colorado Plateau, in: F.R. Boyd,

H.O.A. Meyer (Eds.), The Mantle Sample. Inclusions in Kimberlites and Other Volcanics, AGU, Washington, DC, 1979, pp. 345–356.
[68] D. Smith, Chlorite-rich ultramafic reaction zones in Colorado Plateau xenoliths: recorders of sub-Moho hydration, Contrib. Mineral. Petrol. 121 (1995) 185–200.
[69] D. Smith, Insights into the evolution of the uppermost continental mantle from xenolith localities on and near the Colorado Plateau and regional comparisons, J. Geophys. Res. 105 (2000) 16769–16781.
[70] W.C. Hunter, D. Smith, Garnet peridotite form the Colorado Plateau ultramafic diatremes: hydrates, carbonates, and comparative geothemometry, Contrib. Mineral. Petrol. 76 (1981) 312–330.
[71] H.G. Wilshire, C.E. Meyer, J.K. Nakata, L.C. Calk, J.W. Shervais, J.E. Nielson, E.C. Schwarzman, Mafic and ultramafic xenoliths from volcanic rocks of the Western United States, U. S. Geol. Surv. Prof. Pap. 1443 (1988) (179 pp.).
[72] M.G. Best, Mantle-derived amphibole within inclusions in alkali-basaltic lavas, J. Geophys. Res. 79 (1974) 2107–2113.
[73] M.G. Best, Amphibole-bearing cumulate inclusions Grand Canyon, Arizona and their bearing on silica-undersaturated hydrous magmas in the upper mantle, J. Petrol. 16 (1975) 212–236.
[74] D.W. Matson, D.W. Muenow, M.O. Garcia, Volatiles in amphiboles from xenoliths, Vulcan's Throne, Grand Canyon, Arizona, USA, Geochim. Cosmochim. Acta 48 (1984) 1629–1636.
[75] S.C. Bergman, K.A. Foland, F.J. Spera, On the origin of an amphibole-rich vein in a peridotite inclusion from the Lunar Crater Volcanic Field, Nevada, USA, Earth Planet. Sci. Lett. 56 (1981) 343–361.
[76] K. Righter, I.S.E. Carmichael, Mega-xenocrysts in alkali olivine basalts: fragments of disrupted mantle assemblages, Am. Mineral. 78 (1993) 1230–1245.
[77] R.D. Aines, G.R. Rossman, Water content of mantle garnets, Geology 12 (1984) 720–723.
[78] D.R. Bell, G.R. Rossman, The OH content of "anhydrous" minerals in mantle eclogites, Eos, Trans. Am. Geophys. Union 71 (1990) 523.
[79] D.R. Bell. Hydroxyl in mantle minerals, PhD thesis, California Institute of Technology, 1993, 385 pp.
[80] G.A. Snyder, L.A. Taylor, E.A. Jerde, R.N. Clayton, T.K. Mayeda, P. Deines, G.R. Rossman, N.V. Sobolev, Archean mantle heterogeneity and the origin of diamondiferous eclogites, Siberia: evidence from stable isotopes and hydroxyl in garnet, Am. Mineral. 80 (1995) 799–809.
[81] S.S. Matsyuk, K. Langer, A. Hösch, Hydroxyl defects in garnets from mantle xenoliths of the Siberian platform, Contrib. Mineral. Petrol. 132 (1998) 163–179.
[82] J.F. Luhr, T.B. Housh, Melt volatile contents in basalts from Lathrop Wells and Red Cone, Yucca Mountain region, SW Nevada: insights from glass inclusions, EOS: Trans. Am. Geophys. Union 83 (2002) 47 (Fall Mtg Supp.).
[83] B.E. Hill, S.J. Lynton, J.F. Luhr, Amphibole in quaternary basalts of the Yucca mountain region: significance to volcanism models, Proc. 6th Ann. Int. Conf. High Level Radioactive Waste Management, Las Vegas, Nevada, American Nuclear Society, LaGrange, IL, 1995, pp. 132–134.
[84] J.S. Whitlock, Evidence of a mantle wedge source for slab window volcanism in the northern California Coast Ranges, MSc thesis, Pennsylvania State University, 2002.
[85] M. Liu, K. Furlong, Cenozoic volcanism in California coast ranges: numerical solutions, J. Geophys. Res. 97 (1992) 4941–4951.
[86] R.A. Lange, I.S.E. Carmichael, P.R. Renne, Potassic volcanism near Mono basin, California: evidence for high water and oxygen fugacities inherited from subduction, Geology 21 (1993) 949–952.
[87] S.N. Feldstein, R.A. Lange, Pliocene Potassic magmas from the Kings River region, Sierra Nevada, California: evidence for melting of a subduction-modified mantle, J. Petrol. 40 (1999) 1301–1320.
[88] K. Wang, T. Plank, J.D. Walker, E.I. Smith, A mantle melting profile across the Basin and Range, SW USA, J. Geophys. Res. 107 (2002) (10.1029/2001JB000209).
[89] P.D. Asimow, J.E. Dixon, C.H. Langmuir, A hydrous melting and fractionation model for mid-ocean ridge basalts: Application to the Mid-Atlantic Ridge near the Azores, Geochemistry, Geophysics, Geosystems (2004) doi:10.1029/2003GC000568.
[90] E. Humphreys, E. Hessler, K. Dueker, G. Lang Farmer, E. Erslev, T. Atwater, How Laramide-age hydration of North American Lithosphere by the Farallon slab controlled subsequent activity in the western US, Int. Geol. Rev. 45 (2003) 575–595.
[91] T. Atwater, Plate tectonic history of the northeast Pacific and western North America, Geology of North America, vol. N: Eastern Pacific Ocean and Hawaii, in: E.L. Winterer, D.M. Hussong, R.W. Decker (Eds.), Geol. Soc. Am. Boulder, CO, 1989, pp. 21–72, .
[92] H. Staudigel, S.D. King, Ultrafast subduction: the key to slab recycling efficiency and mantle differentiation? Earth Planet. Sci. Lett. 109 (1992) 517–530.
[93] S. Peacock, Large-scale hydration of the lithosphere above subducting slabs, Chem. Geol. 108 (1993) 49–59.
[94] L.V. Danyushevsky, T.J. Falloon, A.V. Sobolev, A.J. Crawford, M. Carroll, R.C. Price, The H_2O content of basalt glasses from southwest Pacific back-arc basins, Earth Planet. Sci. Lett. 117 (1993) 347–362.
[95] E. Stolper, S. Newman, The role of water in the petrogenesis of Mariana trough magmas, Earth Planet. Sci. Lett. 121 (1993) 293–325.
[96] A.V. Sobolev, M. Chaussidon, H_2O concentrations in primary melts from supra-subduction zones and mid-ocean ridges: implication for H_2O storage and recycling in the mantle, Earth Planet. Sci. Lett. 137 (1996) 45–55.
[97] P. Michael, The concentration, behavior and storage of H_2O in the suboceanic upper mantle: implications for mantle metasomatism, Geochim. Cosmochim. Acta 52 (1988) 555–566.
[98] D. Lizarralde, A. Chave, G. Hirth, A. Schultz, Northeastern Pacific mantle conductivity profile from long-period magne-

totelluric soundings using Hawaii-to-California submarine cable data, J. Geophys. Res. 100 (1995) 17837–17854.
[99] A. Saal, E.H. Hauri, C.H. Langmuir, M. Perfit, Vapor undersaturation in primitive mid-ocean ridge basalt and the volatile content of the Earth's upper mantle, Nature 419 (2002) 451–455.
[100] K. Simons, J.E. Dixon, J.-G. Schilling, R. Kingsley, R. Poreda, Volatiles in basaltic glasses from the Easter–Salas y Gomez Seamount Chain and Easter Microplate: implications for geochemical cycling of volatile elements, Geochem. Geophys. Geosystems (2002) doi:10.1029/2001GC000173.
[101] J.E. Dixon, D.A. Clague, P. Wallace, R. Poreda, Volatiles in alkalic basalts from the North Arch Volcanic Field, Hawaii: Extensive degassing of deep submarine-erupted alkalic series lavas, J. Petrol. 38 (1997) 911–939.
[102] P.J. Wallace, Water and partial melting in mantle plumes: Inferences from the dissolved H_2O concentrations of Hawaiian basaltic magmas, Geophys. Res. Lett. 25 (1998) 3639–3642.
[103] H. Bureau, N. Métrich, M.P. Semet, T. Staudacher, Fluid–magma decoupling in a hot-spot volcano, Geophys. Res. Lett. 26 (1999) 3501–3504.
[104] A.R.L. Nichols, M.R. Carroll, Á. Höskuldsson, Is the Iceland hot spot also wet? Evidence from the water contents of undegassed submarine and subglacial pillow basalts, Earth Planet. Sci. Lett. 202 (1999) 77–87.
[105] M.G. Bostock, R.D. Hyndman, S. Rondenay, S.M. Peacock, An inverted continental Moho and serpentinization of the forearc mantle, Nature 417 (2002) 536–538.
[106] T.M. Brocher, T. Parsons, A.M. Trehu, C.M. Snelson, M.A. Fisher, Seismic evidence for widespread serpentinized forearc upper mantle along the Cascadia margin, Geology 31 (2003) 267–270.
[107] J.E. Dixon, D.A. Clague, Volatiles in basaltic glasses from Loihi Seamount, Hawaii: evidence for a relatively dry plume component, J. Petrol. 42 (2001) 627–634.
[108] J.E. Dixon, L. Leist, C. Langmuir, J.G. Schilling, Recycled dehydrated lithosphere observed in plume-influenced mid-ocean-ridge basalt, Nature 420 (2002) 385–389.
[109] R.J. Stern, Subduction zones, Rev. Geophys. 40 (4) (2002) 1012 (10.1029/2001RG000108).
[110] G. Nolet, A. Zielhuis, Low S velocities under the Tornquist–Teisseyre zone: evidence for water injection into the transition zone by subduction, J. Geophys. Res. 99 (1994) 15813–15820.
[111] M. Van der Meijde, F. Marone, D. Giardini, S. van der Lee, Seismic evidence for water deep in Earth's upper mantle, Science 300 (2003) 1556–1558.
[112] A.L. Boettcher, J.R. O'Neil, Stable isotope, chemical, and petrographic studies of high-pressure amphiboles and micas: evidence for metasomatism in the mantle source regions of alkali basalts and kimberlites, Am. J. Sci. 280A (1980) 594–621.
[113] D.R. Bell, T.C. Hoering, H_2O contents and D/H ratios of mantle amphiboles, Carnegie Inst. Wash. Yearbook 93 (1994) 89–90.
[114] G. Wörner, R.S. Harmon, J. Hoefs, Stable isotope relations in an open magma system, Laacher See, Eifel (FRG), Contrib. Mineral. Petrol. 95 (1987) 343–349.
[115] P.D. Kempton, R.S. Harmon, H.-G. Stosch, J. Hoefs, C.J. Hawkesworth, Open-system O-isotope behaviour and trace element enrichment in the sub-Eifel mantle, Earth. Planet. Sci. Lett. 89 (1988) 273–287.
[116] Y. Kuroda, T. Suzuoki, S. Matsuo, Hydrogen isotope composition of deep seated water, Contrib. Mineral. Petrol. 60 (1977) 311–315.
[117] T. Usui, E. Nakamura, K. Kobayashi, S. Maruyama, H. Helmstaedt, Fate of the subducted Farallon plate inferred from eclogite xenoliths in the Colorado Plateau, Geology 31 (2003) 589–592.
[118] W.R. Dickinson, W.S. Snyder, Geometry of subducted slabs related to San Andreas transform, J. Geol. 87 (1979) 609–627.
[119] P. Bird, Laramide crustal thickening event in the Rocky Mountain foreland and Great Plains, Tectonics 3 (1984) 741–758.
[120] J. Severinghaus, T. Atwater, Cenozoic geometry and thermal state of the subducting slabs beneath western North America, in: B. Wernicke (Ed.), Basin and Range Extension, Geol. Soc. Am., Mem., vol. 176, 1990 pp. 1–22.
[121] S.P. Grand, Mantle shear structure beneath the Americas and surrounding oceans, J. Geophys. Res. (1994) 11591–11621.
[122] E. Humphreys, K. Dueker, Western US upper mantle structure, J. Geophys. Res. 99 (1994) 9615–9634.
[123] S. van der Lee, G. Nolet, Seismic image of the subducted trailing fragments of the Farallon plate, Nature 386 (1997) 266–269.
[124] S. Karato, Mapping water content in the upper mantle, in: J. Eiler (Ed.), Inside the Subduction Factory, Am. Geophys. Union, Geophys. Monograph Ser. 118 (2004) 135–152.
[125] T. Mizukami, S.R. Wallis, J. Yamamoto, Natural example of olivine lattice preferred orientation patterns with a flow-normal *a*-axis maximum, Nature 427 (2004) 432–436.
[126] T.S. James, J.J. Clague, K. Wang, I. Hutchinson, Post-glacial rebound at the northern Cascadia subduction zone, Quat. Sci. Rev. 19 (2000) 1527–1541.
[127] M.I. Billen, M. Gurnis, A low viscosity wedge in subduction zones, Earth Planet. Sci. Lett. 193 (2001) 227–236.
[128] K. Furlong, Thermal–rheological evolution of the upper mantle and the development of the San Andreas fault system, Tectonophys 223 (1993) 149–164.
[129] K. Lambeck, P. Johnston, C. Smither, M. Nakada, Glacial rebound of the British Isles: III. Constraints on mantle viscosity, Geophys. J. Int. 125 (1996) 340–354.
[130] K. Lambeck, C. Smither, P. Johnston, Sea level change, glacial rebound and mantle viscosity for northern Europe, Geophys. J. Int. 134 (1998) 102–144.
[131] A.M. Forte, J.X. Mitrovica, New inferences of mantle viscosity from joint inversion of long wavelength mantle convection and post-glacial rebound data, Geophys. Res. Lett. 23 (1996) 1147–1150.
[132] G. Kaufmann, K. Lambeck, Mantle dynamics, postglacial rebound and the radial viscosity profile, Phys. Earth Planet. Inter. 121 (2000) 303–327.
[133] M. Simons, B. Hager, Localization of the gravity field

and the signature of glacial rebound, Nature 390 (1997) 500–504.
[134] T. Nishimura, W. Thatcher, Rheology of the lithosphere inferred from post-seismic uplift following the 1959 Hebgen Lake earthquake, J. Geophys. Res. 108 (2003) 2389 (10.1029/2002JB002191).
[135] J.X. Mitrovica, A.M. Forte, Radial profile of mantle viscosity: results from the joint inversion of convection and postglacial rebound observables, J. Geophys. Res. 102 (1997) 2751–2769.
[136] K.S. Pitzer, S.M. Sterner, Equations of state valid continuosly from zero to extreme pressures for H_2O and CO_2, J. Chem. Phys. 101 (1994) 3111–3116.
[137] A.G. Hochstaedter, J.B. Gill, M. Kusakabe, S. Newman, M.S. Pringle, B. Taylor, P. Fryer, Volcanism in the Sumisu rift: I. Major element, volatile, and stable isotope geochemistry, the Mariana Trough; special section, Earth Planet. Sci. Lett. 100 (1990) 179–194.
[138] T.W. Sisson, G.D. Layne, H_2O in basalt and basaltic andesite glass inclusions from four subduction-related volcanoes, Earth Planet. Sci. Lett. 117 (1993) 619–635.
[139] P.F. Dobson, H. Skogby, G.R. Rossman, Water in boninite glass and coexisting orthopyroxene; concentration and partitioning, Contrib. Mineral. Petrol. 118 (1995) 414–419.
[140] T. Plank, K. Kelley, Wet melting in the oceanic mantle, EOS Trans. AGU 84 (46) (2003) (Fall Meet. Suppl., Abstract T51H-02).
[141] D.T. Vaniman, B.M. Crowe, E.S. Gladney, Petrology and geochemistry of Hawaiite lavas from Crater flat, Nevada, Contrib. Mineral. Petrol. 80 (1982) 341–357.